HHS Public Access

Author manuscript

Nano Lett. Author manuscript; available in PMC 2019 October 10.

Published in final edited form as:

Nano Lett. 2018 October 10; 18(10): 6449–6454. doi:10.1021/acs.nanolett.8b02917.

Optimization of a Degradable Polymer-Lipid Nanoparticle for Potent Systemic Delivery of mRNA to the Lung Endothelium and Immune Cells

James C. Kaczmarek[1,2], **Kevin J. Kauffman**[1,2], **Owen S. Fenton**[2,3], **Kaitlyn Sadtler**[2], **Asha K. Patel**[1,4], **Michael W. Heartlein**[5], **Frank DeRosa**[5], and **Daniel G. Anderson**[1,2,6,7,*]

[1]Deparment of Chemical Engineering, Massachusetts Institute of Technology, Cambridge, MA (USA)

[2]David H. Koch Institute for Integrative Cancer Research, Massachusetts Institute of Technology, Cambridge, MA (USA)

[3]Department of Chemistry, Massachusetts Institute of Technology, Cambridge, MA (USA)

[4]Division of Cancer and Stem Cells, School of Medicine, University of Nottingham, Nottingham NG7 2RD (UK)

[5]Translate Bio, Lexington, MA (USA)

[6]Institute for Medical Engineering and Science, Massachusetts Institute of Technology, Cambridge, MA (USA)

[7]Harvard and MIT Division of Health Science and Technology, Massachusetts Institute of Technology, Cambridge, MA (USA)

Abstract

mRNA therapeutics hold great potential for treating a variety of diseases through protein-replacement, immunomodulation, and gene editing. However, much like siRNA therapy, the majority of progress in mRNA delivery has been confined to the liver. Previously, we demonstrated that poly(β-amino esters), a class of degradable polymers, are capable of systemic mRNA delivery to the lungs in mice when formulated into nanoparticles with poly(ethylene glycol)-lipid conjugates. Using experimental design, a statistical approach to optimization that reduces experimental burden, we demonstrate herein that these degradable polymer-lipid nanoparticles can be optimized in terms of polymer synthesis and nanoparticle formulation to achieve a multiple order-of-magnitude increase in potency. Furthermore, using genetically

*Correspondence dgander@mit.edu.

Experimental Section

Polymers were synthesized by dissolving diacrylate, amine, and alkyl amine monomers (concentration 1M) in anhydrous N,N-dimethylformamide at various molar ratios for 48 hours at 90°C. End-capping monomer was then added at room temperature and reacted for an additional 24 hours, followed by 2–3 washes with diethyl ether. Polymers were stored at −80 to −20°C and dissolved in DMSO for formulation. Nanoparticles were synthesized by dissolving mRNA in sodium acetate buffer (pH 5.2) and polymer/hydrophobic moieties in ethanol as a separate phase. The two phases were mixed either by hand at a 1:1 v/v ratio or by microfluidic device at a 3:1 aqueous: ethanol v/v ratio. Statistical design and analysis was done using JMP software.

All animal experiments were approved by the MIT Institutional Animal Care and Use Committee and were consistent with local, state, and federal regulations as applicable.

Additional experimental details can be found in the supplementary information.

engineered Cre reporter mice, we demonstrate that mRNA is functionally delivered to both the lung endothelium and pulmonary immune cells, expanding the potential utility of these nanoparticles.

Keywords

mRNA Delivery; Nanoparticles; Polymers; Optimization; PBAE

Recent advances in the synthesis of *in vitro* transcribed (IVT) mRNA have triggered an expansion of research into the delivery of such mRNAs for a variety of therapeutic purposes.[1] For the controlled production of specific proteins *in vivo*, delivery of mRNA is particularly attractive given its transient expression and elimination of risk for genomic insertion compared to DNA.[2] Therapeutic mRNA delivery requires bypassing a number of barriers, including RNAse-mediated degradation, cellular entry, and endosomal escape.[3] Considerable effort has been dedicated to the development of vectors that can transport nucleic acids to target cells *in vivo*.[4,5] Non-viral nanoparticles, in particular, have emerged as promising mRNA delivery vehicles for a variety of applications including immunotherapy[6–9], protein replacement[10–12], and gene editing.[13,14] However, like siRNA, the majority of work has focused on delivery to the liver following systemic delivery.[4,5,11,15–17] Thus, the broadest realization of RNA therapeutics in the clinic requires the development of delivery vehicles capable of potent, specific mRNA delivery to a range of tissues, and, in particular, non-liver organs.

For mRNA delivery, the lungs are a particularly interesting target, given the breadth of disease targets affecting endothelial[18,19], epithelial[20,21], and immune[22,23] pulmonary cells. Schrom *et al.* recently reported the delivery of angiotensin-converting enzyme 2 mRNA to pulmonary cells following systemic delivery; however their precise nanoparticle formulation was not disclosed.[10] Previously, degradable poly(β-amino ester) (PBAE) nanoparticles formulated with poly(ethylene glycol)-lipid (PEG-lipid) were developed and shown to facilitate delivery of mRNA selectively to the lung following systemic administration.[24] Here, we describe the improvement of this system using a design of experiment approach that uses statistical methods to limit necessary experimental conditions.[17] We report a multiple order-of-magnitude increase in potency of mRNA delivery *in vivo*, while maintaining lung specificity.

A key feature of PBAE synthesis is its relative simplicity.[25–27] The reaction proceeds through the Michael addition of an amine to a diacrylate under mild conditions with high conversion.[28] PBAE terpolymers incorporate an additional alkylamine in the backbone (see supporting information for reaction scheme).[29] Previous studies seeking to optimize PBAE nanoparticles have focused on the synthesis of libraries using a diverse set of monomers,[25,30] and altering polymer end-capping,[31] molecular weight,[32] and alkylamine chain length (in the case of terpolymers).[29] We sought to investigate the simultaneous evaluation of such synthesis parameters in the context of a single diacrylate/amine pair. Specifically, we chose to vary the end capping group, the length of the alkylamine carbon chain, the molar ratio of diacrylate to amines (alters the molecular weight[33]), and the molar ratio of the alkylamine to

4-(2-amino methyl) morpholine (Table S1). The diacrylate and amine chosen for this purpose, bisphenol A glycerolate and 4-(2-amino methyl) morpholine, respectively (Fig. 1a), were identified as efficacious in previous studies of terpolymers[29] and were the most effective *in vivo* following formulation with mRNA and PEG-lipid.[24]

Building upon previous studies demonstrating that co-formulating polymer-nucleic acid particles with PEG-lipid can enhance function, we sought to explore utility of PEG-lipids with the materials developed here.[24] Formulation of PEG-lipid with nucleic acid and these materials requires the use of two phases: an organic phase (ethanol) to dissolve the polymer and PEG-lipid, and an acidic aqueous phase (sodium acetate buffer, 25 mM) consisting of the dissolved nucleic acid. These phases must be mixed and then dialyzed against PBS to remove organic solvent and to reach physiological pH. This extra processing makes traditional methods of high-throughput particle synthesis less practical. Thus, instead of performing a full-factorial screen, experimental design was utilized in order to reduce the number of polymers/formulations necessary to explore the design space including all of the variables of interest. This statistical method was previously utilized to optimize lipid nanoparticle formulations[17], but had not before been applied to PBAE synthesis. To this end, JMP software was utilized to design a partial factorial screen of 30 polymers (Table S2) within the parameter space detailed in Table S1. Polymers were synthesized according to a previously reported protocol.[24] Briefly, diacrylate and amine monomers were dissolved in N,N-dimethylformamide with an excess of diacrylate and the step polymerization was allowed to proceed for 48 hours at 90°C. Following polymerization, an excess of end-capping monomer was added and reacted at room temperature for 24 hours. The polymer was then purified via excess monomer removal by multiple washes in diethyl ether.

For formulation, polymers were dissolved in DMSO at 100 mg/mL, and the resulting solution was co-dissolved in ethanol with 7 wt% PEG-lipid, mixed with an equal volume of luciferase-encoding mRNA diluted in 25 mM sodium acetate buffer by pipetting, and dialyzed against PBS.[24] The resulting nanoparticles were used to transfect HeLa cells (0.2 ng/μL mRNA dose), which were assayed for luminescence 24 hours following transfection. As can be seen in Figure 2, several polymers were more potent than the original polymer, with the top-performing variant, referred to hereafter as A1 (Figure 2, red bar), over two orders of magnitude more effective than the original. Importantly, this difference was also observed *in vivo* (Fig. 2, insert), suggesting that in terms of relative efficacy, this *in vitro* screen recapitulated *in vivo* results. The statistical model generated showed that the end cap had the only statistically significant effect on efficacy (Fig. S2). Of these monomers, the end cap used in polymer A1 (“end cap 1”) had the strongest positive correlation with efficacy. End-cap screening alone has already been performed for a large set of PBAE materials[31] and demonstrated that the five used herein are the most effective and as such subsequent synthesis screens were not performed. However, even without subsequent optimization, the potency of the polymer was improved using only a fraction of the available design space, demonstrating the power of experimental design for the rapid optimization of PBAE synthesis.

It is difficult to pinpoint the reason that the A1 structure, and not structurally similar polymers, formed the superior nanoparticle in this study. One previous study showed that

even a single methylene group within a cationic lipid can drastically change transfection potency.[34] Indeed, the DOE methodology herein was chosen since correlating subtle structural properties with efficacy – that is, rational design – for nucleic acid delivery has been difficult.[16,25,35] It is possible that these polymer alterations may affect endosomal escape of the nanoparticles, as this has been hypothesized to be a major limiting step for cytoplasmic delivery of nucleic acid therapeutics.[36,37] Additional studies will be need to better understand the key limiting steps facing cytoplasmic delivery systems.

In addition to optimizing the polymer synthesis, we sought to optimize the nanoparticle formulation, which has been shown to have a significant effect on mRNA delivery.[17] Because the effects of formulation, such as changes in serum stability or biodistribution[24], are not always identifiable *in vitro*, formulation screens were performed *in vivo*. The improvements in delivery through non-covalent formulation of PBAE terpolymers with PEG-lipid[24,29] suggest that incorporation of other hydrophobic moieties may also improve function. As such, we sought to adapt lipid nanoparticle formulation strategies for use with PBAE materials. In particular, we sought to investigate the utility of 1,2-dioleoyl-*sn*-glycero-3-phosphoethanolamine (DOPE) and cholesterol when co-formulated with PBAE polymers.[17] In addition, we altered polymer N/P ratio, the PEG MW in the PEG-lipid, the phospholipid length in the PEG-lipid, and the molar composition of PEG-lipid in the formulation (Fig. 1b).

Given that formulation with these moieties in the context of a PBAE terpolymer nanoparticle had not been reported, the potential design space was exceptionally broad. As such, we utilized a definitive screen, a special three-level screening design useful in narrowing a design space.[38] The parameter ranges chosen can be found in Table S3. Additionally, to ensure proper mixing of all components, these particles were formulated using a microfluidic device that has been shown to consistently synthesize lipid nanoparticles with similar components.[39] As with the *in vitro* screen, we chose to use luciferase-coding mRNA as a reporter, as it would give us a means of quantifying protein production via image analysis while allowing us to visualize the biodistribution of mRNA translation. Synthesized particles were injected intravenously in female C57BL/6 mice (0.5 mg mRNA/kg mouse), and the mouse organs were excised and imaged for luminescence using an IVIS imaging apparatus 24 hours following injection (Fig. S12). As a control, deemed the “base formulation”, A1 polymer was formulated with only mRNA and 7 mol% C14-PEG2000 at the same ratios as used with the non-optimized polymer (“original” polymer in Fig. 2) in previous studies[24]. Figure 3a shows the results of this screen in the lungs and spleen, the two organs where luminescence was most prominent in the control particle (Figure S12). Only one formulation (D2) was more potent than the base formulation, and only one parameter, DOPE mol%, was statistically significant (Fig. S3). However, the goal of the definitive screen was mainly to exclude less important variables.[17]

We based a subsequent partial factorial screen off of a combination of the statistical model obtained from the screen as well as the parameter levels used in the D2 formulation (Figure 3a, Table S3). Specifically, cholesterol and PEG-lipid lipid chain length were eliminated and the remaining parameters were narrowed or altered in range. The parameters for this screen can be seen in Table S5, and a more detailed discussion of how these new parameters were

chosen can also be found in the supporting information. Figure 3b shows that, as one would expect from successive screening, multiple formulations were more potent in the lungs than the base formulation. However, the partial factorial screen revealed several formulations that also transfected the spleen, and the overall lung-specificity of even those particles most effective in the lungs was decreased. To better understand the relationship between formulation and organ-specificity, we looked to the effects of PEG-lipid incorporation, which had a significant effect on both lung and spleen efficacy (Fig. S4–5). Another dependent variable, particle diameter, was also strongly correlated with PEG-lipid incorporation (Fig. S6), so we investigated the relationship between particle size and efficacy. As can be seen in Fig. S7, the nanoparticle formulations can be grouped into two distinct size regions: very small diameter (<100 nm), which corresponded to low efficacy, and large (>300 nm) diameter, which corresponded with high efficacy in both lung and spleen, with the spleen showing particularly consistent efficacy. Previous studies have reported that larger particles tend to be endocytosed by splenocytes[40]. As for small-diameter particles, the two primary parameters exerting significant negative correlation on particle size were PEG MW and PEG-lipid mol%. This, too, is consistent with our data demonstrating that too much PEG-shielding of PBAE nanoparticles ablates their efficacy.[24] We therefore hypothesized that further optimization of PEG-lipid mol% could increase nanoparticle specificity for the lungs. We chose to manipulate PEG-lipid mol%, as it can be altered with higher precision than can the PEG MW, which is limited by the available molecular weights sold commercially.

For this final PEG-lipid content-based screen, we synthesized nanoparticles with an N/P of 50, 20 mol% DOPE, and 1–7 mol% C18-PEG2000. All particles synthesized in this range, which yielded particle diameters within the region of interest (Fig. S8), showed improved lung specificity (Figure 3c). Although formulation L2 (1.5 mol% PEG-lipid) showed the highest efficacy, we chose L3 (5 mol% PEG-lipid) as our optimized, lung-targeting formulation. L3 was not significantly less effective than L2, but it was almost half the size, which our data correlates with generally decreased weight loss following intravenous injection in mice (Fig. S10). Overall, this optimized particle (referred to hereafter as A1-L3) was multiple orders of magnitude more effective than the commercially available *in vivo* jetPEI reagent across multiple doses (Fig. 3d), and did not significantly alter liver enzyme levels at an intermediate dose (Fig. S11). This particle also demonstrated a high degree of lung specificity compared to MD1 (also known as cKK-E12) lipid nanoparticles (Fig. S13).[16,41]

In general, the correlation between nanoparticle size and efficacy is tenuous at best[42], especially when one considers that the particle size measured in solution may not be the same in the context of plasma. Thus, we do not expect that this relationship will be fully translatable to all other mRNA delivery platforms. Nevertheless, for these specific nanoparticles, we identified a correlation between size and lung-specificity (Figs. S6–8, Fig. 3c).

Having identified an optimized, lung-targeting particle, we sought to determine the cell populations within the lungs were being transfected by this formulation. We utilized a mouse line expressing a tdTomato fluorophore cassette containing an upstream Lox-P flanked stop

codon. After administering and expressing Cre-recombinase mRNA, this stop codon can be removed from the cassette, causing the cells which successfully translate Cre to constitutively express tdTomato[43]. Using this method, it is possible to identify - with single cell resolution - those cells to which mRNA is delivered.

A1-L3 nanoparticles were formulated with Cre-encoding mRNA, and delivered intravenously. Forty-eight (48) hours later, the mouse lungs were harvested and processed into a single-cell suspension, and analyzed using multi-color flow cytometry (FACS) analysis. This formulation primarily transfected the lung endothelium, with ~75% of endothelial cells expressing tdTomato (Fig. 4a). The number of immune cells transfected (~2%) was low by comparison (Fig. 4a).[44] As shown in Fig. 4b, the majority of immune cells expressing protein are dendritic cells and various monocytes, although a portion T and B cells were also transfected. (Fig. S16).

In conclusion, we utilized design of experiments to optimize a degradable, polymeric nanoparticle both in terms of polymer synthesis as well as nanoparticle formulation. This methodology allowed us to develop a polymer formulation two orders-of-magnitude more effective than its pre-optimized form *in vitro* and *in vivo* (Fig. 2), and the use of successive formulation screens sequentially increased the efficacy of our nanoparticles while additionally allowing us to identify formulations that maintain lung-specificity (Fig. 3). The utility of these design of experiment methods in the context of a polymeric nanoparticle rather than a lipid nanoparticle further demonstrates its potential for *in vivo* optimization of RNA delivery vehicles.[17] We envision that the use of experimental design *in vivo* may also be used to optimize nanoparticles for other organs as well. Moreover, the high level of mRNA expression in the lungs, coupled with these particles' ability to transfect pulmonary endothelial and immune cells (Fig. 4) suggests that these particles may be useful in a variety of therapeutic contexts.

Supplementary Material

Refer to Web version on PubMed Central for supplementary material.

Acknowledgements

The authors would like to acknowledge project funding by Translate Bio (Lexington, MA), in addition to partial funding from the Cancer Center Support (core) Grant P30-CA14051 from the NCI. The authors acknowledge the contribution of the Koch Institute Nanotechnology Materials Core, Animal Imaging and Preclinical Testing Core, and Flow Cytometry Core.

References

(1). Kaczmarek JC; Kowalski PS; Anderson DG Genome Med 2017, 9, 60. [PubMed: 28655327]

(2). Yamamoto A; Kormann M; Rosenecker J; Rudolph C Eur. J. Pharm. Biopharm 2009, 71 (3), 484–489. [PubMed: 18948192]

(3). Dowdy SF Nat. Biotechnol 2017, 35 (3), 222–229. [PubMed: 28244992]

(4). Kauffman KJ; Webber MJ; Anderson DG J. Control. Release 2016, 240, 227–234. [PubMed: 26718856]

(5). Guan S; Rosenecker J Gene Ther 2017, 24 (3), 133–143. [PubMed: 28094775]

(6). Pardi N; Secreto AJ; Shan X; Debonera F; Glover J; Yi Y; Muramatsu H; Ni H; Mui BL; Tam YK; et al. Nat. Commun 2017, 8, 14630. [PubMed: 28251988]

(7). Stadler CR; Bähr-Mahmud H; Celik L; Hebich B; Roth AS; Roth RP; Karikó K; Türeci Ö; Sahin U Nat. Med 2017, No. December 2016, 3–8.

(8). Su X; Fricke J; Kavanagh DG; Irvine DJ Mol. Pharm 2011, 8 (3), 774–787. [PubMed: 21417235]

(9). Chahal JS; Khan OF; Cooper CL; McPartlan JS; Tsosie JK; Tilley LD; Sidik SM; Lourido S; Langer R; Bavari S; et al. Proc. Natl. Acad. Sci 2016, 113 (29), E4133–E4142. [PubMed: 27382155]

(10). Schrom E; Huber M; Aneja M; Dohmen C; Emrich D; Geiger J; Hasenpusch G; Herrmann-Janson A; Kretzschmann V; Mykhailyk O; et al. Mol. Ther. - Nucleic Acids 2017, 7 (June), 350–365. [PubMed: 28624211]

(11). DeRosa F; Guild B; Karve S; Smith L; Love K; Dorkin JR; Kauffman KJ; Zhang J; Yahalom B; Anderson DG; et al. Gene Ther 2016, 23 (10), 699–707. [PubMed: 27356951]

(12). Mahiny AJ; Dewerth A; Mays LE; Alkhaled M; Mothes B; Malaeksefat E; Loretz B; Rottenberger J; Brosch DM; Reautschnig P; et al. Nat. Biotechnol 2015, 33 (6), 584–586. [PubMed: 25985262]

(13). Yin H; Song C-Q; Dorkin JR; Zhu LJ; Li Y; Wu Q; Park A; Yang J; Suresh S; Bizhanova A; et al. Nat. Biotechnol 2016, 34 (3), 328–333. [PubMed: 26829318]

(14). Miller JB; Zhang S; Kos P; Xiong H; Zhou K; Perelman SS; Zhu H; Siegwart DJ Angew. Chemie Int. Ed 2017, 56 (4), 1059–1063.

(15). Kanasty R; Dorkin JR; Vegas A; Anderson D Nat. Mater 2013, 12 (11), 967–977. [PubMed: 24150415]

(16). Fenton OS; Kauffman KJ; McClellan RL; Appel EA; Dorkin JR; Tibbitt MW; Heartlein MW; DeRosa F; Langer R; Anderson DG Adv. Mater 2016, 28 (15), 2939–2943. [PubMed: 26889757]

(17). Kauffman KJ; Dorkin JR; Yang JH; Heartlein MW; DeRosa F; Mir FF; Fenton OS; Anderson DG Nano Lett 2015, 15 (11), 7300–7306. [PubMed: 26469188]

(18). Green CE; Turner AM Respir. Res 2017, 18 (1), 20. [PubMed: 28100233]

(19). Leus NGJ; Morselt HWM; Zwiers PJ; Kowalski PS; Ruiters MHJ; Molema G; Kamps JAAMInt. J. Pharm 2014, 469 (1), 121–131. [PubMed: 24746643]

(20). Bals R; Hiemstra PS Eur. Respir. J 2004, 23 (2), 327–333. [PubMed: 14979512]

(21). Griesenbach U; Alton EWFWHum. Mol. Genet 2013, 22 (R1), R52–8. [PubMed: 23918661]

(22). Kim EY; Battaile JT; Patel AC; You Y; Agapov E; Grayson H; Benoit LA; Byers DE; Alevy Y; Tucker J; et al. Nat. Med 2008, 14 (6), 633–640. [PubMed: 18488036]

(23). Grumelli S; Corry DB; Song L; Song L; Green L; Huh J; Hacken J; Espada R; Bag R; Lewis DE; et al. PLoS Med 2004, 1 (1), e8. [PubMed: 15526056]

(24). Kaczmarek JC; Patel AK; Kauffman KJ; Fenton OS; Webber MJ; Heartlein MW; DeRosa F; Anderson DG Angew. Chemie Int. Ed 2016, 55 (44), 13808–13812.

(25). Anderson DG; Lynn DM; Langer R Angew. Chemie Int. Ed 2003, 42 (27), 3153–3158.

(26). Cutlar L; Zhou D; Gao Y; Zhao T; Greiser U; Wang W; Wang W Biomacromolecules 2015, 16 (9), 2609–2617. [PubMed: 26265425]

(27). Gao Y; Huang J; O'Keeffe Ahern J; Cutlar L; Zhou D; Lin F-H; Wang W Biomacromolecules 2016, 17 (11), 3640–3647. [PubMed: 27641634]

(28). Lynn DM; Langer RJ Am. Chem. Soc 2000, 122 (44), 10761–10768.

(29). Eltoukhy A. a.; Chen D; Alabi C. a.; Langer R; Anderson DG Adv. Mater 2013, 25, 1487–1493. [PubMed: 23293063]

(30). Shmueli RB; Sunshine JC; Xu Z; Duh EJ; Green JJ Nanomedicine Nanotechnology, Biol. Med 2012, 8 (7), 1200–1207.

(31). Zugates GT; Peng W; Zumbuehl A; Jhunjhunwala S; Huang Y-H; Langer R; Sawicki J. a; Anderson DG Mol. Ther 2007, 15 (7), 1306–1312.

(32). Eltoukhy A. a.; Siegwart DJ; Alabi C. a.; Rajan JS; Langer R; Anderson DG Biomaterials 2012, 33, 3594–3603. [PubMed: 22341939]

(33). Fourth Odian, G..; John Wiley & Sons, Inc.: Hoboken, NJ, 2004.

(34). Jarzębińska A; Pasewald T; Lambrecht J; Mykhaylyk O; Kümmerling L; Beck P; Hasenpusch G; Rudolph C; Plank C; Dohmen C Angew. Chemie - Int. Ed 2016, 55 (33), 9591–9595.

(35). Sunshine JC; Akanda MI; Li D; Kozielski KL; Green JJ Biomacromolecules 2011, 12 (10), 3592–3600. [PubMed: 21888340]

(36). Sahay G; Querbes W; Alabi C; Eltoukhy A; Sarkar S; Zurenko C; Karagiannis E; Love K; Chen D; Zoncu R; et al. Nat. Biotechnol 2013, 31 (7), 653–658. [PubMed: 23792629]

(37). Gilleron J; Querbes W; Zeigerer A; Borodovsky A; Marsico G; Schubert U; Manygoats K; Seifert S; Andree C; Stöter M; et al. Nat. Biotechnol 2013, 31 (June), 638–646. [PubMed: 23792630]

(38). Jones B; Nachtsheim CJ J. Qual. Technol 2011, 43 (1), 1–15.

(39). Chen D; Love KT; Chen Y; Eltoukhy AA; Kastrup C; Sahay G; Jeon A; Dong Y; Whitehead KA; Anderson DG J. Am. Chem. Soc 2012, 134 (16), 6948–6951. [PubMed: 22475086]

(40). Blanco E; Shen H; Ferrari M Nat. Biotechnol 2015, 33 (9), 941–951. [PubMed: 26348965]

(41). Dong Y; Love KT; Dorkin JR; Sirirungruang S; Zhang Y; Chen D; Bogorad RL; Yin H; Vegas AJ; Alabi CA; et al. Proc. Natl. Acad. Sci 2014, 111 (15), 5753–5753.

(42). Whitehead K. a; Matthews J; Chang PH; Niroui F; Dorkin JR; Severgnini M; Anderson DG ACS Nano 2012, 6, 6922–6929. [PubMed: 22770391]

(43). Kauffman KJ; Oberli MA; Dorkin JR; Hurtado JE; Kaczmarek JC; Bhadini S; Wyckoff J; Langer R; Jaklenec A; Anderson DG Mol. Ther. - Nucleic Acids 2017, 10 (March), 55–63. [PubMed: 29499956]

(44). Bantikassegn A; Song X; Politi K Am. J. Respir. Cell Mol. Biol 2015, 52 (4), 409–417. [PubMed: 25347711]

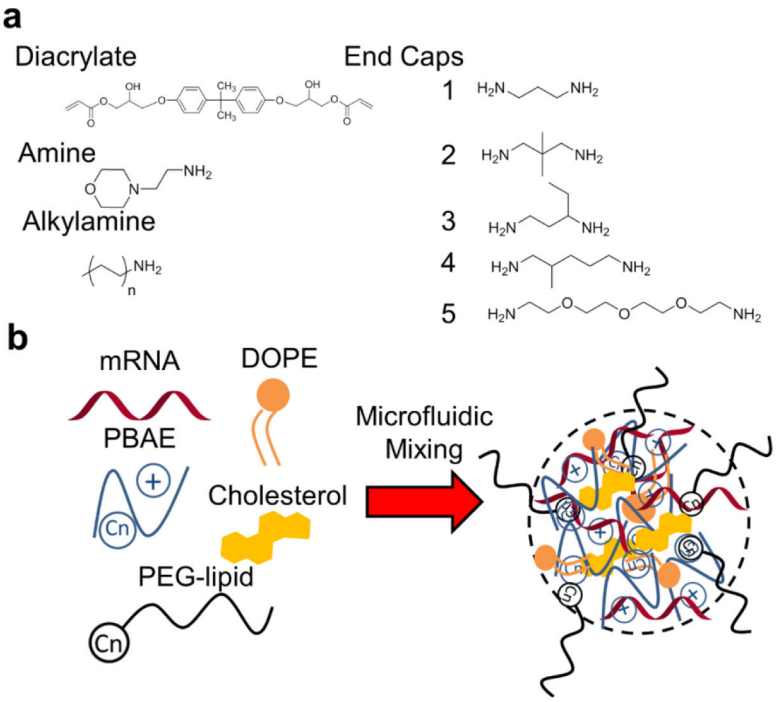

Figure 1.

a) Monomers used in synthesis screen for PBAE terpolymers, based on previous reports[24,29,31]. The diacrylate and amines step-polymerize via Michael addition, and can be end-capped in a separate step by keeping the diacrylate in excess during polymerization.[31]

b) Schematic depicting the formulation moieties used in formulation screen for *in vivo* mRNA delivery. mRNA binds with the polymer on the basis of its cationic charge, while the alkylamine in the polymer provides a non-covalent handle for hydrophobic moieties to incorporate into the nanoparticle.

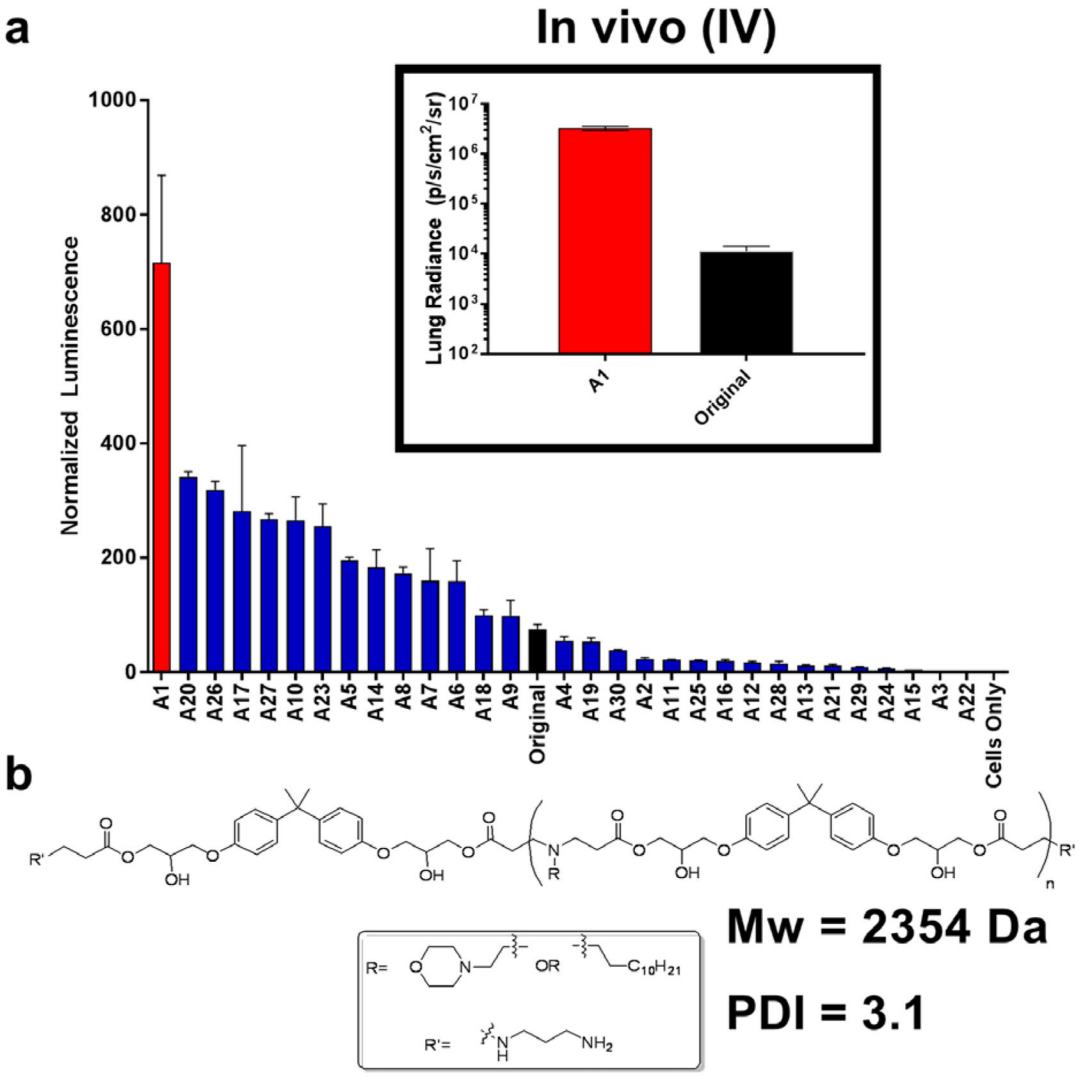

Figure 2.

(a) A partial factorial screen optimizing PBAE synthesis parameters reveals several polymers more potent than the original when delivered *in vitro* in HeLa cells *(n*=4*)*. **(insert)** The top-performing polymer, A1 (red), is two orders of magnitude more potent *in vivo* in mouse lungs after IV delivery than the original, corresponding well to the *in vitro* results (*n*=3). All particles were synthesized with luciferase-coding mRNA at an N/P of 57 with 7 wt% C14-PEG2000 PEG-lipid.[24] Note: 10^2 used as minimum in insert to account for magnitude of background luminescence. **(b)** Structural identity of A1 polymer.

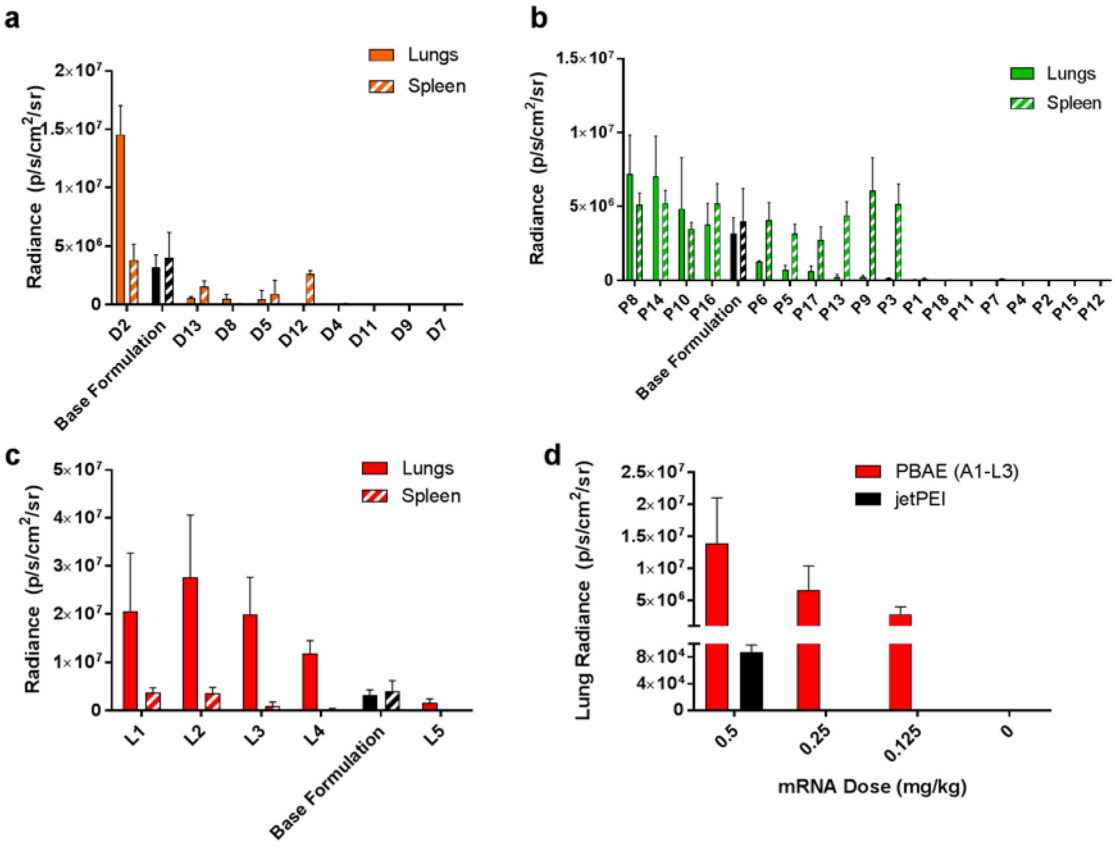

Figure 3.

Luciferase-encoding mRNA was delivered via A1 PBAE nanoparticles intravenously in mice, and luminescence in various organs was assessed at 24 hours. **a)** A definitive screen revealed one formulation that was more potent than the base formulation (i.e. A1 polymer with 7 mol% C14-PEG2000 PEG-lipid). This formulation, along with statistical data from the screen, was used to develop the parameter space for a subsequent partial factorial screen. **b)** The partial factorial screen had a greater number of formulations more potent in the lung (22% vs. 7%), but several formulations showed high luciferase signal in the spleen. **c)** By optimizing the mol% of PEG-lipid in the formulation, high lung-specificity could be obtained. **d)** The optimized PBAE polymer/formulation (A1-L3) is orders of magnitude more potent than jetPEI across multiple mRNA doses (n=3 for all experiments).

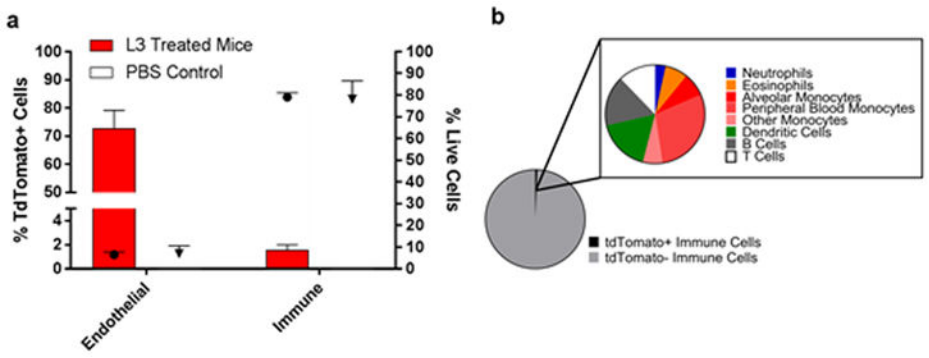

Figure 4.

Analysis of lung cell types transfected using Ai14 Cre/lox reporter mice. **a)** Percentages of cell types that were TdTomato+ (bars, left axis), indicating successful transfection with Cre mRNA using A1-L3 nanoparticles. Symbols (● for treated mice, ▼ for control mice, right axis) represent percentages of live cells which were either endothelial or immune cells (n = 3). **b)** Identification of immune cell (CD45+) subtypes which express tdTomato following delivery of Cre mRNA via A1-L3 nanoparticles in Ai14 mice (n = 2).